STATISTICAL, NONLINEAR, AND SOFT MATTER PHYSICS

One-Dimensional Photonic Crystals with a Planar Oriented Nematic Layer: Temperature and Angular Dependence of the Spectra of Defect Modes

V. G. Arkhipkin[a,b]*, V. A. Gunyakov[a,b], S. A. Myslivets[a], V. P. Gerasimov[a],
V. Ya. Zyryanov[a,b], S. Ya. Vetrov[b], and V. F. Shabanov[a]

[a] *Kirenskii Institute of Physics, Siberian Branch, Russian Academy of Sciences,*
Akademgorodok, Krasnoyarsk, 660036 Russia
*e-mail: avg@iph.krasn.ru
[b] *Siberian Federal University, Krasnoyarsk, 660041 Russia*
Received May 18, 2007

Abstract—Transmission spectra of a one-dimensional photonic crystal (PC) formed by two multilayer dielectric mirrors and a planar oriented layer of 5CB nematic liquid crystal (LC) that is sandwiched between these mirrors and serves as a structure defect are investigated experimentally. Specific features of the behavior of the spectrum of defect modes as a function of the angle of incidence of light on the crystal are studied for two polarizations: parallel and perpendicular to the director of the LC; the director either lies in the plane of incidence or is perpendicular to it. It is shown that, for the configurations considered, the maxima of the defect modes shift toward the short-wavelength region as the tilt angle of incidence radiation increases; this tendency is more manifest for the parallel-polarized component, when the director lies in the plane of incidence. In the latter case, the width of the photonic band gap (PBG) appreciably decreases. The temperature dependence of the polarization components of the transmission spectra of a PC is investigated in the case of normal incidence of light. The spectral shift of defect modes due to the variation of the refractive index of the LC at the nematic–isotropic liquid phase transition point is measured. It is shown that, in real PCs, the amplitude of defect modes decreases when approaching the center of the band gap, as well as when the number of layers in the dielectric mirrors increases. Theoretical transmission spectra of the PCs calculated by the method of recurrence relations with regard to the decay of defect modes are in good agreement with experimental data.

PACS numbers: 42.70.Qs, 78.20.Ci, 42.82.Et

DOI: 10.1134/S1063776108020179

1. INTRODUCTION

Materials whose permittivity varies periodically in one, two, or three directions on a spatial scale comparable to the wavelength of light are called photonic crystals (PCs), or photonic crystal structures. Sometimes, these structures are called superlattices. They attract considerable interest as new optical materials because they possess unique properties [1–3]. An important property of PCs is the presence of photonic band gaps (PBGs), or stop bands, with low density of photon states and a low transmittance (or large reflectivity) in some directions of propagation of light. In three-dimensional PCs, there may exist complete PBGs, in which light of any polarization cannot propagate in any direction at certain frequencies of light [1, 4]. Photonic band gaps are characterized by extraordinary dispersive properties, which allow one to realize light propagation regimes in photonic crystal structures, that are interesting from the physical point of view and important for applications [5, 6].

In a PC with a lattice defect, i.e., with broken periodicity, transmission bands arise in the band gaps, which are also called defect, or localized, modes and whose position and transmittance can be controlled by varying the geometric and structural parameters [3]. In this case, light is localized in the vicinity of a defect; this increases the intensity of light wave inside the defect layer. Photonic crystal materials with defects made it possible to develop new types of waveguides—photonic crystal waveguides [6, 7], high-Q nanoresonators [8, 9], and low-threshold lasers [9, 10]. In [11–14], methods are proposed for increasing the efficiency of nonlinear optical processes. The development of the component base for optoelectronics and information technology is discussed in [2].

One-dimensional PCs represent multilayer periodic structures consisting of alternating layers of two dielectric materials with different refractive indices [1–3]. In contrast to three-dimensional PCs, they do not have a complete PBG; however, they attract considerable interest in view of their multifunctionality. Note that the production technique of one-dimensional PCs for the

optical range is well developed [2]. These structures have long been investigated and widely used as interference filters, light polarizers, multilayer dielectric reflectors, and antireflecting coatings [7, 15, 16]. At present, multilayer structures are investigated within the concept of PCs. This approach provides a new insight into the optical properties of PCs and allows one to increase their applicability, including the applications to the observation of new physical effects and phenomena. For example, giant birefringence was observed in multilayer polymer structures [17], and reflectors with high reflectivity in a wide frequency range virtually for any angle of incidence of light with arbitrary polarization (omnidirectional reflectors) [18] and wideband filters whose transmission band does not depend on the angle of incidence (omnidirectional transmission) [19] were proposed. In [20], the authors discuss the possibility of designing photonic-crystal heterostructures with a narrow frequency and sharp angular defect mode. One-dimensional PCs are used for fabricating lasers [21] and nonlinear optical converters [22]. Recently, a method, based on PCs, for controlling the group velocity of pulses was proposed, and the possibility of recording, storing, and reading optical information was considered [23].

Photonic crystals with tunable spectral characteristics attract considerable interest. In this relation, PCs that contain liquid crystal (LC) layers as their structural elements are quite promising. The properties of LCs, such as a wide transmission range (0.4–3.0 μm), high optical birefringence Δn ($|\Delta n|$ can be as high as 0.2–0.8), large nonlinearity, and high sensitivity to external fields (temperature and electric and magnetic fields) [24] make LCs a quite promising means for the effective control of the spectral and optical characteristics of PCs [2, 3, 25]. Originally, LCs for controlling the spectral properties of PCs were proposed in [26, 27]. Intensive investigations of PCs in combination with LCs started in 1999 (see [2, 25]). The thermal tuning of PBGs in PCs with infiltrated LCs was demonstrated in opal [28], porous silicon [29], and a two-dimensional Ga–As PC [30]. The temperature tuning of the spectrum of defect modes at a wavelength of about 1 μm in planar photonic crystal microresonators was implemented in [31]. The electrical tuning of defect modes in a one-dimensional PC with a nematic LC as a defect layer, as well as wavelength tunable lasing was demonstrated in [32–34]. Compact tunable lasers based on a two-dimensional PC with an LC-filled microresonator are demonstrated in [35] (see also references in [35]).

Theoretical analysis of the spectrum of defect modes and the field distribution in defect modes, associated with the anisotropy of a nematic LC considered as a structural defect layer of a one-dimensional PC was carried out in [36]. The properties of electric-field-tuned transmission spectra of two-dimensional dielectric and metal PCs that contain liquid-crystal materials as defect elements or layers were investigated in [37]. In [38], the authors proposed a tuned-wavelength

reflector for any tilt angle of incidence of light; this reflector is based on a PC consisting of alternating isotropic and LC layers, and the tuning is performed by an external electric field.

Investigations of PCs based on porous silicon with pores filled with an LC are of great interest (see, for example, [39–41]). In such photonic crystal structures, thermal and electrical modulation of transmission bands was performed at the frequencies of defect modes [42], and electrically tuned active reflectors were produced [43]. The thermal and electrical tuning of the spectral characteristics by means of LCs was also realized in photonic crystal waveguides [44].

The anisotropy of PCs determines not only the polarization optical properties of PCs but also the position of a band gap [41, 45, 46]. The properties of LC-containing PCs depend on the orientation of the director of the LC. The optical measurements of the transmittance (reflectivity) as a function of temperature, polarization, and angle of incidence allow one to investigate the configuration of the director field [47]; this opens up possibilities for the optimization of the characteristics of PCs.

A review of literature on the subject shows that the thermal tuning of the transmission (reflection) spectrum of LC-containing PCs has generally been realized in two- and three-dimensional PCs. The analysis of this phenomenon in one-dimensional PCs is of independent interest, because these PCs are widely used in various optical devices. Recently, we experimentally investigated thermooptical switching of defect modes ($\Delta\lambda = 10$ nm) in a one-dimensional PC with a defect layer of a homeotropically oriented nematic LC [48] and studied the effect of the tilt angle of incident radiation on the transmission spectrum of defect modes in such a crystal [49]. The angular dependence of a PBG in the one-dimensional periodic structure Si/SiO_2 for infrared radiation was investigated in [50]. The present paper has been motivated by the fact that there is no experimental investigations of the spectral properties of one-dimensional PCs with an LC defect as a function of temperature for various angles of incidence and various polarizations of light waves. A variable angle of incidence is a convenient parameter for tuning the frequency of defect modes. Combined with an LC, this parameter allows one to extend the possibilities of controlling the spectra of PCs. The aim of the present paper is the experimental investigation and theoretical analysis of the effect of temperature and angle of incidence of light on the spectrum of defect modes of a PC when the optical axis of the nematic LC forming a defect layer is directed along the plane of multilayers (planar orientation). In this case, in view of the birefringence of the LC, the spectrum of defect modes splits into two polarization components for an arbitrary polarization of incident radiation; when the angle of incidence deviates from the normal direction, one should consider at least four configurations of optical measurements, depend-
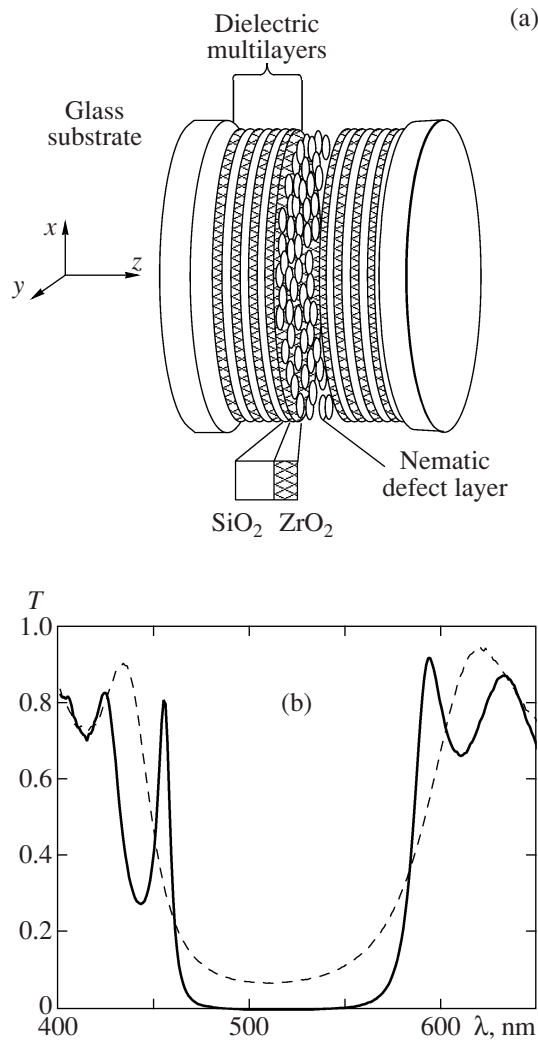
Fig. 1. (a) Schematic view of the structure of a one-dimensional multilayer PC with a nematic defect layer at its center. (b) Transmission coefficients of individual multilayer mirrors as a function of the light wavelength under normal incidence: the solid line corresponds to a mirror with eleven layers of ZrO_2 and ten layers of SiO_2; the minimal transmission at the center of the band gap is about 0.003. The dashed line corresponds to a mirror with six layers of ZrO_2 and five layers of SiO_2; the minimal transmission is about 0.07.

ing on the orientations of the electric field of the light wave and the director of the LC. We investigate the specific features of the transmission spectra in all four cases. We also analyze the effect of losses on the propagation of light in such a PC.

2. EXPERIMENT

2.1. Structure and Parameters of a PC

The structure of the PC under investigations is expressed as $(HL)^N H(D)H(LH)^N$. Here, H and L are optically isotropic dielectric layers with high and low

refractive indices n_1 and n_2 and thicknesses t_1 and t_2, respectively; the period of the lattice is $t = t_1 + t_2$. D is a defect layer with refractive index n_d and thickness t_d. N is the number of bilayers HL and LH (the number of periods). The defect layer is filled with a 4-n-pentyl-4'-cyanobiphenyl (5CB) planar oriented nematic LC, which is characterized by the following series of phase transitions from solid-crystalline, nematic, and isotropic-liquid states: C–22.5°C–H–34.0°C–I.

Figure 1a represents the schematic view of the structure of the PC. Two identical multilayer mirrors are assembled into a sandwich-like plane-parallel cell and are placed in a temperature-controlled chamber. The gap t_d between the mirrors (the thickness of the defect layer) is specified by teflon spacers. Each mirror consists of $N + 1$ layers of zirconium dioxide (ZrO_2) with a refractive index of $n_1 = 2.04$ and N layers of silicon dioxide (SiO_2) with a refractive index of $n_2 = 1.45$, which were deposited by turns on the surface of a glass substrate. The values of the refractive indices $n_{1,2}$ (and of the liquid crystal n_{LC} below) correspond to a wavelength of $\lambda = 589$ nm. Figure 1b represents the transmission spectra of two types of mirrors with different numbers of layers that are used in our measurements. Figure 1 shows that there is a band gap in the transmission spectrum of an individual mirror. The maximal reflection occurs at the center of the band gap an smoothly falls off toward its edges. The increase of the number of bilayers from five to ten leads to the decrease of the transmission at the center of the stop band by more than a factor of 20.

To obtain a homogeneous planar oriented nematic LC in the defect layer, we layered, as a surfactant, 1% aqueous solution of polyvinyl alcohol on the working surfaces of the mirrors. The polymer film obtained was subjected to unidirectional rubbing. The cell thus obtained was filled with a nematic LC heated to temperature of 36°C. The quality of the planar orientation of samples was controlled by appropriate texture patterns under conoscopic observation with the use of a polarizing microscope.

The temperature-controlled chamber allowed one to measure the transmission spectra of a PC in the temperature interval 20–40°C to within a stabilization accuracy of ±0.2°C. Polarized transmission spectra were measured by a KSVU-23 spectrometer. As a polarizing element, we used a polyvinylene polaroid with a polarization degree of $p \approx 99.97\%$.

Figure 2 represents the transmission spectra of two PCs with LC defect layer recorded under the normal incidence of light polarized parallel to the director of the LC. Figure 2a corresponds to the first sample, which has the following parameters: $t_1 = 55$ nm, $t_2 = 102$ nm, the thickness of the defect layer is $t_d = 2.4$ μm, and $N = 10$; Fig. 2b corresponds to the second sample, which has the parameters $t_1 = 52$ nm, $t_2 = 102$ nm, $t_d = 2.2$ μm, and $N = 5$. In both cases these parameters allow one to form photonic band gaps in the visible spectrum with

defect modes whose amplitudes, number, and position depend on the thickness and the refractive index of the defect layer, the number of layers in the multilayer mirrors, and the losses in the mirrors. Note that the defect modes attain their maximal amplitude near the edges of the band gap. The increase of the number of layers in the mirrors leads to the decrease of the optical transmission in the defect modes; the sharpest decrease of the amplitudes of these modes occurs at the center of the PBG. A similar effect was observed in [33–35]. Unlike the authors of [34], we associate such behavior of defect modes with the fact that real PCs have losses, as will be shown below.

2.2. Angular Dependence of the Transmission Spectra of PCs

To measure the transmission spectra for different angles of incidence of light on the crystal, the cell was placed in a chamber that was designed so that to allow for the rotation of a sample around the axis perpendicular to the propagation direction of incident radiation (the y-axis in Fig. 1a). The tilt angle θ of the incident beam was fixed with an accuracy of at least $\pm 0.5°$. The angular dependence of optical transmission through the PC was measured at a fixed temperature of $T = 23.0 \pm 0.2°C$.

One should expect that, due to the optical anisotropy of the LC layer, the optical transmission of the PC will exhibit different behavior when subjected to radiation with transverse electric (TE) and transverse magnetic (TM) polarizations. By TE polarization is meant a polarization of a light wave such that the electric vector **E** oscillates in the direction perpendicular to the plane of incidence (xz). If the vector **E** oscillates in the plane xz, then a wave has TM polarization. Under the normal incidence of light on a PC with the planar orientation of nematic LC molecules, there are four possible independent mutual orientations of the electric-filed vector **E** and the director **n** of the LC with respect to the coordinate axes; we denote them as XX, XY, YX, and YY (Fig. 3). Here the first symbol refers to the orientation of the electric-field vector, and the second, to the orientation of the LC director; the first two combinations correspond to TM polarization, and the last two, to TE polarization. Figure 3 shows that, for the components XX and XY, the orientation of the electric-field vector **E** with respect to the coordinate axes varies when the direction of the incident light deviates from the normal to the PC. Nevertheless, we will use the notation introduced even for oblique incidence.

When a sample with the nematic director **n** along the y-axis is irradiated by a wave with TE (TM) polarization, we detect the YY (XY) component of transmission; in this case, an extraordinary (ordinary) wave propagates in the defect layer irrespective of the angle of incidence of the wave. In both cases, the refractive index of the defect layer remains invariant under the rotation of the sample and equal to the refractive index
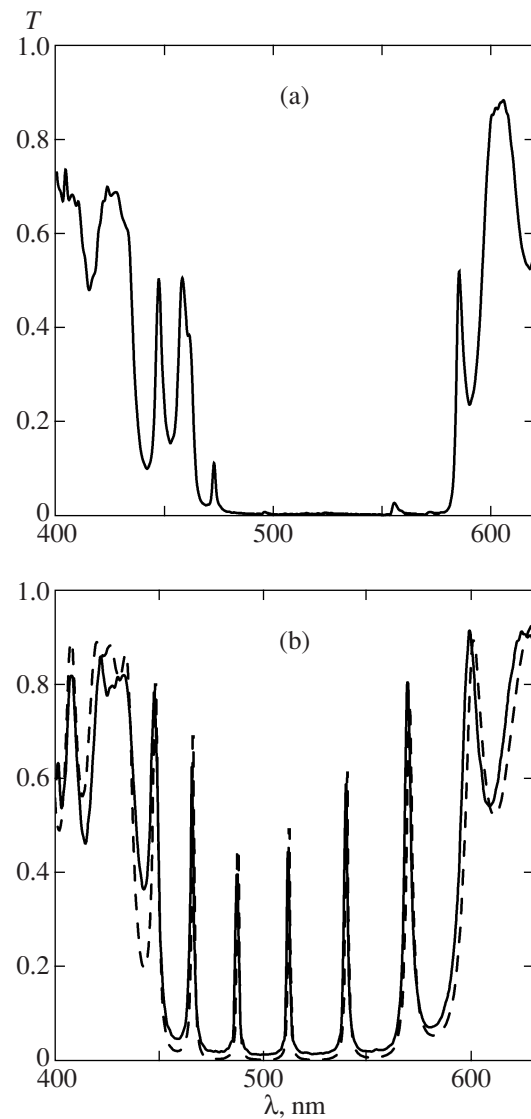

Fig. 2. Transmission spectra of a PC with an LC defect layer: (a) $N = 10$ and (b) 5; the solid line represents the experimental data and the dashed line, the results of calculations.

of the LC, $n_\parallel = n_e$ ($n_\perp = n_o$), where $n_\parallel$ and $n_\perp$ are the refractive indices for light with the polarization parallel and perpendicular to the LC director, and n_e and n_o are the refractive indices for extraordinary and ordinary waves. When a wave with TM polarization is incident on a sample oriented along the x-axis (the XX component), the effective refractive index n_e of the LC defect layer is a function of the angle θ_0 between the wave vector **k** of the light wave in the LC and the local direction of the director **n**. In all four variants, the variation of the tilt angle of the incident wave leads to the variation of the optical path difference of the interfering beams in the PC, which, in turn, leads to the modification of its transmission spectrum. An important feature of the
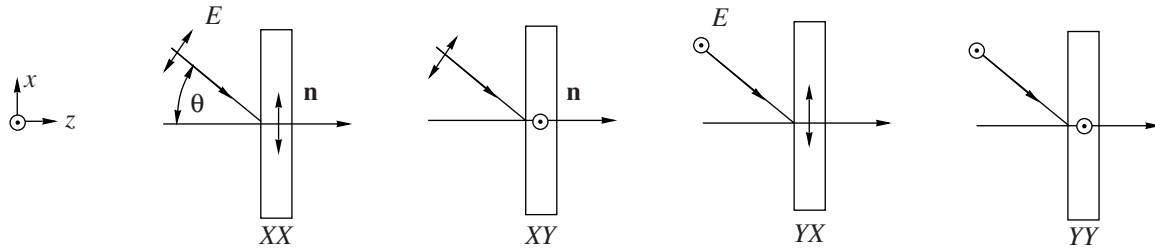
Fig. 3. Relative orientation of the electric vector **E** (*i*) of light passing through a PC and the director **n** (*j*) in the transmission components T_{ij}.

phenomena that arise under oblique incidence of probing radiation is the fact that the nematic layer inside the PC is not strained, as it occurs in the case of reorientation of the director by an electric field. For a fixed angle of incidence θ, the angle θ_0 remains constant across the

Fig. 4. Transmission spectra of a PC with a planar oriented layer of 5CB nematic LC for various angles of incidence θ for (a) TM- (*XX*-) and (b) TE- (*YY*-) polarizations of the incident light; $t_d = 2.2$ μm.

nematic layer; this fact facilitates the analysis of light propagation through the photonic crystal structure. Note also that the case corresponding to the *YX* component is analogous to the case of homeotropic orientation of the LC director, which was considered in [48].
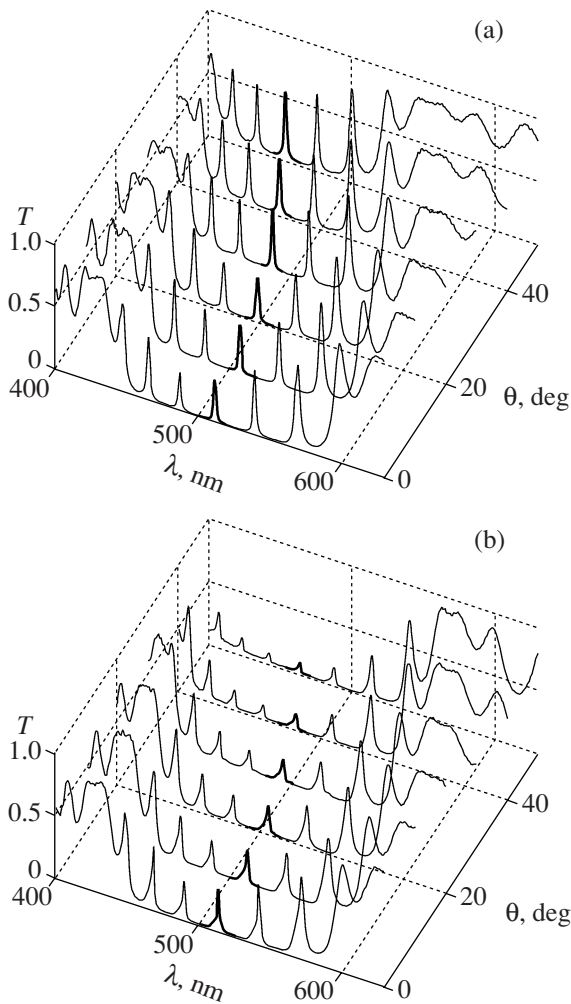
Figure 4 shows, as an example, the transmission spectra of the PC for TM (the *XX* component; Fig. 4a) and TE (*YY* component; Fig. 4b) polarizations of light as a function of the tilt angle θ of incident radiation. For the other two combinations, the spectra are similar. Figure 4 shows that the boundaries of the band gap shift to the short-wavelength region as the angle of incidence increases. In the first case (*XX*), the band gap width appreciably decreases, whereas, in the second case (*YY*), the band gap width remains virtually constant. As the angle of incidence increases, for TE polarization the amplitudes of defect modes decrease, whereas, for TM polarization, these amplitudes increase. This is associated with the fact that, starting from a certain angle of incidence, the reflection coefficient of light with TM polarization becomes less than that for TE polarization. Then, according to formula (17), which describes the transmission of a Fabry–Perot interferometer at the transmission maximum, the transmission coefficient of a TM wave is greater than that of a TE wave, under the assumption that losses are the same in both cases.

2.3. Temperature Dependence of the Spectrum of Defect Modes

In the case of normal incidence of light on a PC with a planar oriented defect layer, one can measure the transmission components $T_{\|, \perp, i}$, where the subscripts "$\|$," "$\perp$," and "i" indicate the direction of the electric-field vector **E**: ($\|$) means that **E** is parallel to the director **n**, ($\perp$) means that **E** is perpendicular to **n**, and "i" denotes that the defect layer is an isotropic liquid.

Figure 5 shows the experimental transmission spectra for a light wave with the polarization perpendicular ($T_\perp$) and parallel ($T_\|$) to the director of the LC under the normal incidence of light on the sample at various temperatures. A comparison with Fig. 4 shows that the increase of the thickness of the defect layer does not affect the parameters of the band gap but leads to the increase of the number of defect modes in the layer. In

the nematic phase, the defect modes exhibit an appreciable shift as temperature increases; this shift is associated with the monotonic increase of the refractive index of 5CB. For the perpendicular component, the shift occurs to the long-wavelength region; for the parallel component, the shift is to the short-wavelength region. For clarity, one of the modes in Fig. 5 is shown by a heavy line. In the neighborhood of the nematic–isotropic phase transition point, the refractive index of the LC experiences a jump [24]. Figure 5 shows that the defect modes corresponding to the nematic phase (solid lines) also experience a steplike shift when heated to the isotropic state (dotted lines) by about 10 nm for the perpendicular component and by 20 nm for the parallel component.

3. SIMULATION OF THE OPTICAL TRANSMISSION OF A ONE-DIMENSIONAL PHOTONIC CRYSTAL

To carry out a simulation of the optical transmission, we use the notation of the structure parameters of the PC that were introduced at the beginning of Subsection 2.1 and are shown in Fig. 6. Below we will assume that the structure is bounded by vacuum from the left and right ($n = \sqrt{\varepsilon} = 1$) and that a plane monochromatic light wave is incident on the PC at angle θ.

When the LC director **n** is parallel either to the x- or y-axis in the laboratory frame, the dielectric tensor of the LC has the form

$$\varepsilon = \begin{pmatrix} \varepsilon_\parallel & 0 & 0 \\ 0 & \varepsilon_\perp & 0 \\ 0 & 0 & \varepsilon_\perp \end{pmatrix} \text{ and } \varepsilon = \begin{pmatrix} \varepsilon_\perp & 0 & 0 \\ 0 & \varepsilon_\parallel & 0 \\ 0 & 0 & \varepsilon_\perp \end{pmatrix}$$

for the XX (YX) and YY (XY) components, respectively; $\varepsilon_\perp = n_\perp^2$ and $\varepsilon_\parallel = n_\parallel^2$ are components of the dielectric constant that are perpendicular and parallel to the director, respectively.

Under an oblique incidence of light on the PC, Maxwell's equations for a monochromatic TM wave of frequency ω in an anisotropic defect layer in the steady-state approximation are expressed as [3]

$$\left[\frac{d^2}{dz^2} - \beta \left(k^2 - \frac{\varepsilon_{zz}\omega^2}{c^2} \right) \right] H_y = 0, \qquad (1)$$

$$E_x = -\frac{ic}{\omega\varepsilon_{xx}} \frac{dH_y}{dz}, \quad E_z(z) = -\frac{kc}{\varepsilon_{zz}\omega} H_y(z), \qquad (2)$$

where c is the speed of light in vacuum, $k = k_x = (\omega/c)n\sin\theta$ is the propagation constant along the x-axis, and $\beta = \varepsilon_{xx}/\varepsilon_{zz}$. Here $\varepsilon_{xx} = \varepsilon_\parallel$ and $\varepsilon_{yy} = \varepsilon_{zz} = \varepsilon_\perp$ are the components of the dielectric tensor in the principal axes. Equations (1) and (2) are written under the assumption that the director of the LC is parallel to the PC layers.
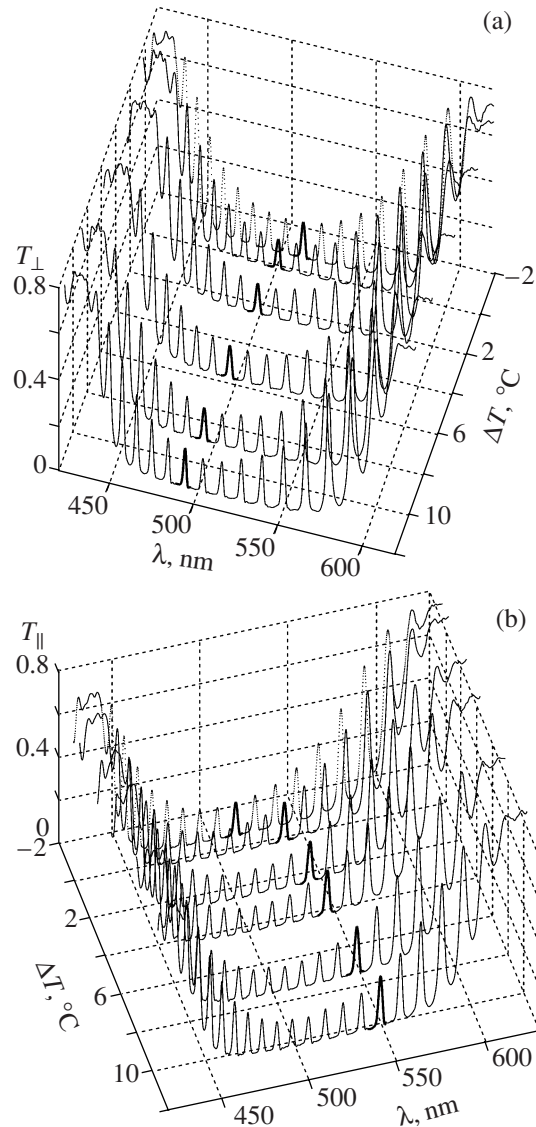

Fig. 5. Transmission spectra of the polarized components (a) $T_\perp$ and (b) $T_\parallel$ of a PC with a planar oriented defect layer in the nematic (solid lines) and isotropic (dotted lines) phases of 5CB at various temperatures: $t_1 = 52$ nm, $t_2 = 102$ nm, $t_d = 6.7$ μm, $N = 5$, $\Delta T = T_c - T$, where T_c is the temperature of phase transition.
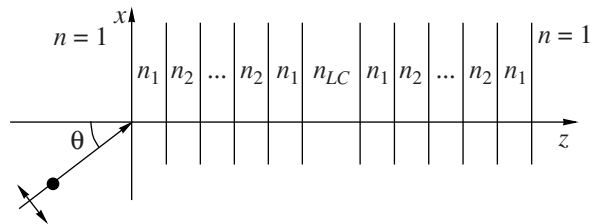

Fig. 6. Schematic view of the one-dimensional photonic crystal structure with an LC layer as a defect.

The corresponding equations for a TE wave are obtained by the following substitutions: $H_y \longrightarrow E_y$, $E_x \longrightarrow H_x$, $E_z \longrightarrow H_z$, and $\varepsilon_{xx} \longrightarrow \varepsilon_{yy}$.

According to Eq. (1), the field $H_y = H$ in an arbitrary jth layer can be represented as a superposition of two counter-propagating waves:

$$H_{(j)} = A_{(j)}\exp[i\alpha_j(z - z_j)] \\ + B_{(j)}\exp[-i\alpha_j(z - z_j)], \quad (3)$$

where $A_{(j)}$ and $B_{(j)}$ are the amplitudes of the forward (incident) and backward (reflected) waves. In the anisotropic defect layer, α_j is expressed as

$$\alpha_j = \sqrt{\varepsilon_{xx}\left(\frac{\omega^2}{c^2} - \frac{k^2}{\varepsilon_{zz}}\right)}. \quad (4)$$

The first equation in (2) gives the following expression for the distribution of the electric field $E_x = E$ in the defect layer:

$$E_j(z) = q_j A_j \exp[i\alpha_j(z - z_j)] \\ - q_j B_j \exp[-i\alpha_j(z - z_j)]. \quad (5)$$

Here,

$$q_j = \sqrt{\frac{\varepsilon_{zz} - n^2\sin^2\theta}{\varepsilon_{xx}\varepsilon_{zz}}}. \quad (6)$$

The formulas for α_j and q_j can be rewritten in the following convenient form:

$$\alpha_{XX}^{TM} = \frac{\omega}{c}\frac{n_\parallel}{n_\perp}\sqrt{n_\perp^2 - \sin^2\theta}, \\ q_{XX}^{TM} = \frac{\sqrt{n_\perp^2 - \sin^2\theta}}{n_\perp n_\parallel}, \quad (7)$$

$$\alpha_{YY}^{TE} = \frac{\omega}{c}\sqrt{n_\parallel^2 - \sin^2\theta}, \quad q_{YY}^{TE} = \sqrt{n_\parallel^2 - \sin^2\theta}, \quad (8)$$

$$\alpha_{XY}^{TM} = \frac{\omega n_\perp}{c n_\parallel}\sqrt{n_\parallel^2 - \sin^2\theta}, \\ q_{XY}^{TM} = \sqrt{\frac{n_\parallel^2 - \sin^2\theta}{n_\perp n_\parallel}}, \quad (9)$$

$$\alpha_{YX}^{TE} = \frac{\omega}{c}\sqrt{n_\perp^2 - \sin^2\theta}, \quad q_{YX}^{TE} = \sqrt{n_\perp^2 - \sin^2\theta}. \quad (10)$$

Equations for isotropic layers are obtained from (1) and (2) by replacing ε_{zz} and ε_{xx} by ε_1 and ε_2 for $E_z = 0$. In this case, α_i and q_i take the form

$$\alpha_i = \frac{\omega}{c}(n_{1,2}^2 - \sin^2\theta)^{1/2}, \\ q_i = \frac{(n_{1,2}^2 - \sin^2\theta)^{1/2}}{n_{1,2}^2}. \quad (11)$$

The boundary conditions require that the tangential components of the vectors **H** and **E** be continuous across the interface.

In contrast to [51], we investigate the transmission spectrum of a PC with an LC defect by the method of recurrence relations [52], which allows us to easily take into account losses in the PC when calculating the reflection and transmission coefficients by introducing complex refractive indices in each layer. Let us divide all the layers of the PC into a sufficiently large number M of sublayers such that the field H_m in each sublayer m can be assumed constant. The continuity of the electric and magnetic components of the fields across the interface between layers m and $m + 1$ yields the following system of equations for the amplitudes of the fields in adjacent layers:

$$A_m + B_m = g_{m+1}^{-1}A_{m+1} + g_{m+1}B_{m+1}, \quad (12)$$

$$q_m(A_m - B_m) \\ = q_{m+1}(g_{m+1}^{-1}A_{m+1} - g_{m+1}B_{m+1}), \quad (13)$$

where $g_m = \exp(i\alpha_m t_m)$, $m = 1, 2, \ldots, M + 1$; $t_m = z_{m+1} - z_m$; and the thickness of the last layer is $t_{M+1} \equiv 0$. The function g_m takes into account the phase change of light waves and their decay in the mth layer.

Let us introduce amplitude reflection coefficients $R_m = B_m/A_m$. From Eqs. (12) and (13) one can easily derive a recurrence relation for the coefficients R_m and R_{m+1} in adjacent sublayers:

$$R_m = \frac{r_m + g_{m+1}^2 R_{m+1}}{1 + r_m g_{m+1}^2 R_{m+1}}. \quad (14)$$

Here, $r_m = (q_m - q_{m+1})/(q_m + q_{m+1})$. Using this recurrence relation and taking into account the boundary condition $R_{M+1} = 0$, we can determine all values of R_m starting from the right boundary of the PC. Then, using Eq. (14), we obtain the following expression for A_{m+1} in terms of A_m in an arbitrary layer m:

$$A_{m+1} = A_m \frac{1 + R_m}{g_{m+1}^{-1} + g_{m+1}R_{m+1}}. \quad (15)$$

Using (15), we find all A_m starting from the left boundary of the PC. Then, we determine the amplitude of the backward wave $B_m = A_m R_m$. The transmission, reflection, and extinction coefficients are given by

$$T = \frac{|A_{M+1}|^2}{|A_0|^2}, \quad R = \frac{|B_0|^2}{|A_0|^2}, \quad A = 1 - T - R, \quad (16)$$

respectively.

4. DISCUSSION OF THE RESULTS

Now, we pass on to the discussion of the experimental results.

The behavior of defect modes in Fig. 2 can be qualitatively understood by using the analogy between a one-dimensional PC with a defect and a Fabry–Perot interferometer. It is well known that the transmission of an interferometer depends substantially on the transmittance T_m (reflectivity R_m) and the loss factor A_m of the mirrors [53]. In the case of identical mirrors, the transmittance of the Fabry–Perot interferometer $T = I_t/I_0$ (I_0 is the intensity of light at the input of the interferometer, and I_t is the intensity of transmitted light) is given by the formula

$$T = \frac{T_m^2}{(T_m + A_m)^2 + 4R_m \sin^2(\delta/2)}, \qquad (17)$$

where $\delta = 4\pi L n_d/\lambda$ is the phase delay due to a double pass of the interferometer (resonator), $L = t_d$ is the resonator base, and n_d is the refractive index of the medium that fills the resonator (the defect layer). Note that the coefficients T_m, A_m, and R_m depend on the wavelength of light.

Since there exist several loss mechanisms (see, for example, [54]), by A_m is meant the effective loss factor determined from the relation $R_m + T_m + A_m = 1$. The parameter A_m strongly influences the transmittance T of the interferometer. Formula (17) shows that, in the absence of losses ($A_m = 0$), $T = 1$ at the transmission maximum for all modes of the resonator irrespective of the wavelength. Due to the losses ($A_m > 0$), this coefficient decreases to

$$T = \frac{T_m^2}{(T_m + A_m)^2} = \frac{1}{(1 + A_m/T_m)^2} < 1. \qquad (18)$$

It follows from (18) that, at the center of the band gap, where T_m is less than at the edges (see Fig. 1), the transmittance of the interferometer attains its minimal value, while the reflectivity attains its maximal value. In this case, the larger the number of layers in the mirrors, the smaller the transmittance T.

Thus, losses in photonic crystal structures may significantly reduce the amplitudes of defect modes. In real PCs, losses may be caused by various factors. The most important role is played by the roughness of the interface between layers; nonparallelism and irregularity of layers (fluctuations of the layer thickness), which lead to the scattering of light; nonresonant absorption in the layers; and other factors. These factors may be crucial for the determination of the spectral properties of defect modes in PCs.

The losses can effectively be taken into account by introducing an imaginary part of the refractive index of each layer, which is related to the effective extinction coefficient (in each layer) κ_j; the latter coefficient determines the decay of the field amplitude when a wave propagates in a PC ($H_j \sim \exp(-\kappa_j z)$). The values of the imaginary parts of the refractive indices (or the extinction coefficients) can be chosen by comparing experi-
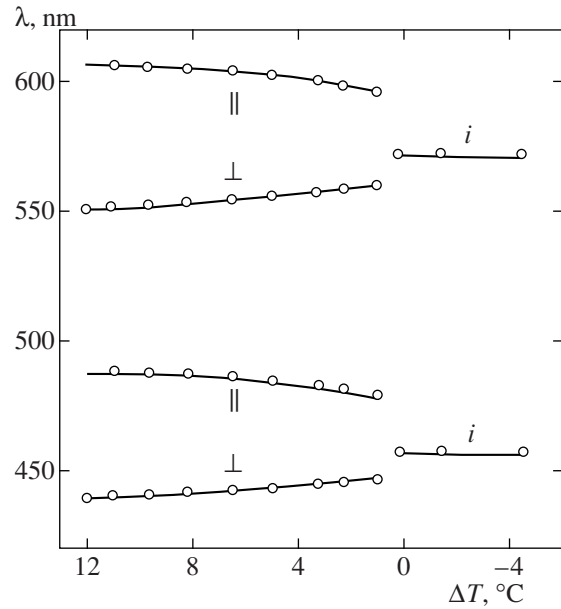

Fig. 7. Positions of the maxima of the short- and long-wavelength defect modes as a function of reduced temperature $\Delta T = T_c - T$. The solid lines correspond to theoretical data, and the circles represent experimental data.

mental data with the results of calculations. Figure 2b shows the calculated and experimental transmission spectra of a PC with an LC defect layer. Good agreement between the calculated and experimental spectra is obtained for the values $\mathrm{Im}\,n_{1,2} = 2 \times 10^{-3}$ and $\mathrm{Im}\,n_{LC} = 1.5 \times 10^{-4}$. These results are obtained with regard to the dispersion of the refractive index in each layer [55–57]. We used these results to simulate the transmission spectra of the system under investigation.

Figure 7 represents the measured and calculated temperature dependence of the maximum-transmission wavelength for two defect modes. One can see that, within the existence region of a mesophase, defect modes smoothly shift, as temperature increases, to the short-wavelength region of the spectrum in the case of parallel polarization and to the long-wavelength region in the case of perpendicular polarization. This feature of the defect modes is attributed to the fact that the refractive indices of 5CB for ordinary and extraordinary waves exhibit different behavior with increasing temperature: the refractive index for an extraordinary wave decreases as temperature increases, while that for an ordinary wave increases [55].

At the point of nematic–isotropic phase transition, which occurs at temperature of $T_c \approx 34°C$, one can observe a steplike shift of modes. The perpendicular component shifts by about 10 nm to the long-wavelength region of the spectrum, while the parallel component shifts by 20 nm to the short-wavelength region. Further heating leads to an insignificant variation in the position of the transmission maxima of defect modes because of the weak temperature dependence of the
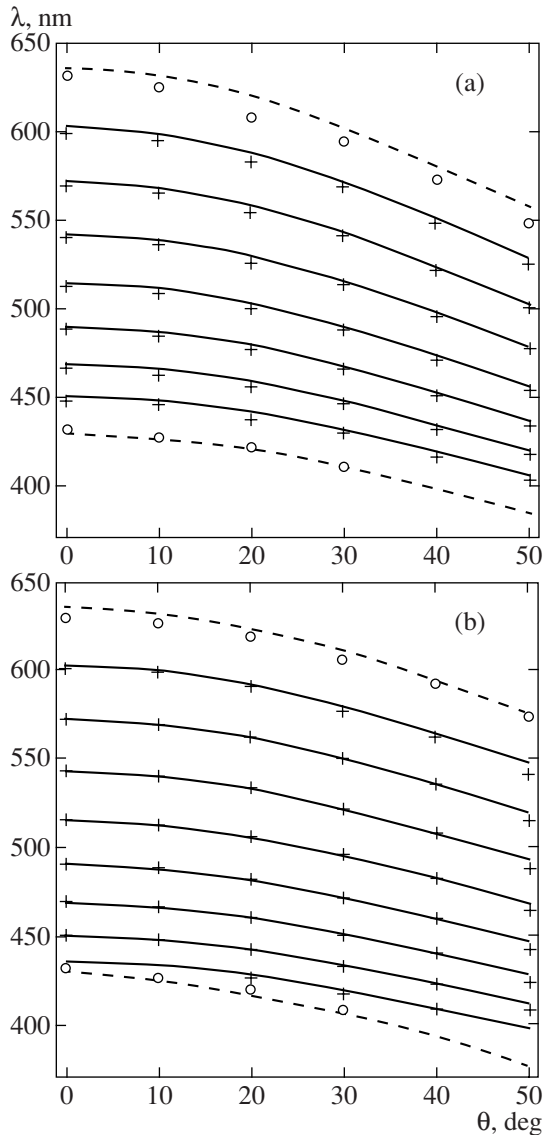
Fig. 8. Computed angular dependence of the spectral positions of the maxima of defect modes (solid lines) and the band gap edges (dashed lines) for (a) TM- (*XX*-) and (b) TE- (*YY*-) polarizations of light incident on the PC. The symbols correspond to the experimental data: $N = 5$ and $t_d = 2.2$ μm.

refractive index of the LC in the isotropic phase. One can see good agreement between the experimental and computed values of the spectral positions of modes over the entire range of temperatures considered.

Figure 8 shows the computed angular dependence of the maximum-transmission wavelengths of defect modes and the band gap edges for TM (a) and TE (b) polarizations. The symbols show the corresponding experimental data, which agree well with the computed data. One can see that the band gap width remains virtually constant (about 200 nm) for TE waves over the entire range of angles θ, whereas, for TM wave, it appreciably narrows down from 200 nm for the normal

incidence of light to 175 nm for $\theta = 50°$. The qualitative difference in the behavior of the band gap edges and the defect modes can also be understood on the basis of the analogy with a Fabry–Perot interferometer. This difference is associated with the different nature of the Fresnel reflection of TE- and TM-polarized light waves from the interfaces between layers. While the reflection coefficient for TE polarization increases with the angle of incidence, for TM polarization it decreases as the angle of incidence increases up to the Brewster angle [58]. At this angle, the Fresnel reflection of TM-polarized light from the interfaces vanishes; this should lead to the decrease of the band gap width to zero. In spite of the fact that there is no Brewster angle for the values of the refractive index of the photonic crystal structure considered, Figs. 4 and 8 show that this tendency is manifest for TM polarization.

Qualitatively, the behavior of defect modes can be explained as follows. As the angle of incidence of light increases, the optical path difference δ of the beams reflected from the interfaces between the defect layer and the multilayer mirrors,

$$\delta = 2Ln_{LC} = \begin{cases} 2L\sqrt{n_\parallel^2 - \sin^2\theta} & \text{for TE waves} \\[2mm] 2L\dfrac{n_\parallel}{n_\perp}\sqrt{n_\perp^2 - \sin^2\theta} & \text{for TM waves} \end{cases}$$

decreases. Then, according to the condition $\delta = l\lambda$ for interference maxima (defect modes), where l is the mode number and λ is its wavelength, this leads to the decrease of the wavelength of the defect mode. Since $n_\parallel > n_\perp$ for the 5CB LC, the optical path difference for TM waves varies faster than that for TE waves as the angle of incidence increases; this, in turn, leads to a faster shift of TM modes (see Fig. 8).

5. CONCLUSIONS

The experimental and theoretical investigations of the temperature and angular dependence of the transmission spectra of one-dimensional PCs with planar oriented LC defect layer carried out in this paper have revealed a number of important features associated with the anisotropy of the dielectric constant of the LC and its sensitivity to temperature, as well as with the decay of the light wave.

We have established experimentally that defect modes attain their maximal amplitude near the edges of a band gap, while at the center of the stop band the optical transmission in the defect modes decreases. In contrast to the authors of [34], we associate this behavior with the decay of light waves propagating in a PC. In the numerical analysis of the transmission spectra, to effectively take into account losses, we introduced complex refractive indices of all layers. On this way we obtained good agreement with experimental results.

As temperature increases, the defect modes recorded for parallel orientation of the electric-field vector **E** of the light wave with respect to the director **n** of the nematic liquid shift to the short-wavelength region of the spectrum; i.e., these modes show a tendency opposite to that of a PC with homeotropic defect texture [48]. The spectral shift of defect modes for the extraordinary wave during the phase transition of the LC to an isotropic liquid is twice that for the ordinary wave; this fact is associated with a similar relation between the jump of the refractive index $n_\parallel$ and that of $n_\perp$ for calamite nematics.

We have experimentally investigated polarization transmission spectra for four orientations of the electric-field vector of a light wave with respect to the director of the LC under the variation of the tilt angle of incident radiation. In all cases, the increase of the angle of incidence leads to the shift of the band gap and the maxima of defect modes to the short-wavelength region of the spectrum. The amplitudes of defect modes may either decrease or increase, depending on the polarization of the incident light. We have shown that, in a one-dimensional PC, a band gap exists in a wide range of angles of incidence. This angle can be used as an effective tuning parameter for shifting the resonance frequency of a defect mode.

The results obtained can also be applied to PCs with different optically uniaxial materials that form structural defects, for example, with uniaxially ordered polymer films, uniaxial smectic LCs, etc.

ACKNOWLEDGMENTS

REFERENCES

1. J. D. Joannopoulos, R. D. Meade, and J. N. Winn, *Photonic Crystals: Molding the Flow of Light* (Princeton Univ. Press, Princeton, N.J., 1995).

2. *Photonic Crystals: Advances in Design, Fabrication, and Characterization*, Ed. by K. Busch, R. B. Wehrspohn, S. Lölkes, and H. Föll (Wiley, Berlin, 2004).

3. V. F. Shabanov, S. Ya. Vetrov, and A. V. Shabanov, *Optics of Real Photonic Crystals. Mesomorphic Defects, Irregularities* (Sib. Otd. Ross. Akad. Nauk, Novosibirsk, 2005) [in Russian].

4. V. P. Bykov, Zh. Éksp. Teor. Fiz. **62**, 505 (1972) [Sov. Phys. JETP **35**, 269 (1972)].

5. Yu. S. Kivshar and G. P. Agrawal, *Optical Solitons: From Fibers to Photonic Crystals* (Academic, Amsterdam, 2003; Fizmatlit, Moscow, 2005).

6. A. M. Zheltikov, Usp. Fiz. Nauk **170**, 1203 (2000) [Phys. Usp. **43**, 1125 (2000)].

7. A. Yariv and P. Yeh, *Optical Waves in Crystals: Propagation and Control of Laser Radiation* (Wiley, New York, 1984; Mir, Moscow, 1987).

8. J. Vučkovic, M. Lončar, H. Mabuchi, et al., Phys. Rev. E **65**, 016608 (2001).

9. Y. Akahane, T. Asano, B. S. Song, et al., Nature **425**, 944 (2003).

10. O. Painter, R. Lee, A. Yariv, et al., Science **284**, 1819 (1999).

11. B. M. Shi, Z. Jiang, X. F. Zhou, et al., J. Appl. Phys. **91**, 6769 (2002).

12. M. G. Martem'yanov, T. V. Dolgova, and A. A. Fedyanin, Zh. Éksp. Teor. Fiz. **125**, 527 (2004) [JETP **98**, 463 (2004)].

13. M. Soljačič and J. D. Joannopoloulos, Nature Mater. **3**, 211 (2004).

14. F. Wang, S. N. Zhu, K. F. Li, et al., Appl. Phys. Lett. **88**, 071102 (2006).

15. M. Born and E. Wolf, *Principles of Optics*, 4th ed. (Pergamon, Oxford, 1969; Nauka, Moscow, 1970).

16. T. N. Krylova, *Interference Covers* (Mashinostroenie, Leningrad, 1973) [in Russian].

17. M. F. Weber, C. A. Stover, L. R. Gilbert, et al., Science **287**, 2451 (2000).

18. Y. Fink, J. N. Winn, S. Chen, et al., Science **282**, 1679 (1998).

19. A. Mandatory, C. Sibilia, M. Bertolotti, et al., J. Opt. Soc. Am. B **22**, 1785 (2005).

20. G. Liang, P. Han, and H. Wang, Opt. Lett. **29**, 192 (2004).

21. J. P. Dowling, M. Scalora, M. J. Bloemer, and Ch. M. Bowden, J. Appl. Phys. **75**, 1896 (1994).

22. N. Mattiucci, G. D'Aguanno, M. J. Bloemer, et al., Phys. Rev. E **72**, 066612 (2005).

23. Z. S. Yang, N. H. Kwong, R. Binder, et al., J. Opt. Soc. Am. B **22**, 2144 (2002).

24. L. M. Blinov, *Electro-Optical and Magneto-Optical Properties of Liquid Crystals* (Nauka, Moscow, 1978; Wiley, New York, 1983).

25. H. Kitzerow, Liq. Cryst. Today **11**, 3 (2002).

26. S. Ya. Vetrov and A. V. Shabanov, Zh. Éksp. Teor. Fiz. **101**, 1341 (1992) [Sov. Phys. JETP **74**, 719 (1992)].

27. K. Busch and S. John, Phys. Rev. Lett. **83**, 967 (1999).

28. K. Yoshino, Y. Shimoda, Y. Kawagishi, et al., Appl. Phys. Lett. **75**, 932 (1999).

29. S. W. Leonard, J. P. Mondia, H. M. van Dreal, et al., Phys. Rev. B **61**, R2389 (2001).

30. Ch. Schuller, F. Klopf, J. P. Reithmaier, et al., Appl. Phys. Lett. **82**, 2767 (2003).

31. B. Wild, R. Ferrini, R. Houdre, et al., Appl. Phys. Lett. **84**, 846 (2004).

32. R. Ozaki, T. Matsui, M. Ozaki, and K. Yoshino, Jpn. J. Appl. Phys. **41**, L1482 (2002).

33. R. Ozaki, T. Matsui, M. Ozaki, and K. Yoshino, Electron. Commun. Jpn., Part 2: Electron. **87**, 24 (2004).

34. R. Ozaki, T. Matsui, M. Ozaki, et al., Appl. Phys. Lett. **82**, 3593 (2003).

35. B. Maune, J. Witzens, Th. Baehr-Jones, et al., Opt. Express **13**, 4699 (2005)

36. S. Ya. Vetrov and A. V. Shabanov, Zh. Éksp. Teor. Fiz. **120**, 1126 (2001) [JETP **93**, 977 (2001)].

37. E. Kosmidou, E. E. Kriezis, and Th. D. Tsiboukis, IEEE Quantum Electron. **41**, 657 (2005).

38. Y.-R. Ha, Y.-C. Kim, and H. Y. Park, Appl. Phys. Lett. **79**, 15 (2001).

39. M. Haurylau, S. P. Andersen, K. L. Marshall, et al., Appl. Phys. Lett. **88**, 061103 (2006).

40. S. M. Weiss, M. Haurylau, and Ph. M. Fauchet, Opt. Mater. **27**, 740 (2005).

41. G. Mertens, Th. Roder, H. Mattias, et al., Appl. Phys. Lett. **15**, 3036 (2003).

42. S. M. Weiss, H. Ouyang, J. Zhang, et al., Opt. Express **13**, 1090 (2005).

43. S. M. Weiss and Ph. M. Fauchet, Phys. Status Solidi A **197**, 556 (2003).

44. T. T. Larsen, A. Bjarklen, D. S. Hermann, et al., Opt. Express **11**, 2589 (2003).

45. Ch. Schuller, J. P. Reithmaier, J. Zimmermann, et al., Appl. Phys. Lett. **87**, 121105 (2005).

46. G. Alagappan, X. W. Sun, P. Shum, et al., J. Opt. Soc. Am. B **23**, 159 (2006).

47. R. Ferrini, J. Marz, L. Zuppiroli, et al., Opt. Lett. **31**, 1238 (2006).

48. V. A. Gunyakov, V. P. Gerasimov, S. A. Myslivets, et al., Pis'ma Zh. Tekh. Fiz. **32** (11), 76 (2006) [Tech. Phys. Lett. **32**, 951 (2006)].

49. S. A. Myslivets, V. A. Gunyakov, V. P. Gerasimov, et al., Dokl. Akad. Nauk **413**, 36 (2007) [Dokl. Phys. **52**, 134 (2007)].

50. H. Högström and C. G. Ribbing, Opt. Commun. **271**, 148 (2007).

51. S. Ya. Vetrov, A. V. Shabanov, and E. V. Shustitskiĭ, Opt. Spektrosk. **100**, 454 (2006) [Opt. Spectrosc. **100**, 409 (2006)].

52. V. A. Bushuev and A. D. Pryamikov, Kvantovaya Élektron. (Moscow) **33**, 515 (2003).

53. W. Demtröder, *Laser Spectroscopy: Basic Concepts and Instrumentation* (Springer, New York, 1981; Nauka, Moscow, 1985).

54. J. Faist, J.-D. Ganiere, Ph. Buffat, et al., J. Appl. Phys. **66**, 1023 (1989).

55. V. Ya. Zyryanov and V. Sh. Épshteĭn, Prib. Tekh. Éksp., No. 2, 164 (1987).

56. I. H. Malitson, J. Opt. Soc. Am. **55**, 1205 (1965).

57. D. L. Wood and K. Nassau, Appl. Opt. **21**, 2978 (1982).

58. S. A. Akhmanov and S. Yu. Nikitin, *Physical Optics* (Mosk. Gos. Univ., Moscow, 1998; Clarendon, Oxford, 1997).

Translated by I. Nikitin